Int J Clin Exp Med 2019;12(4):3569-3579
www.ijcem.com /ISSN:1940-5901/IJCEM0079055

Original Article

The application of qualitative shear wave elastography in differential diagnosis of thyroid nodules

Qian-Qi Liu[1], Zhuo-Wen Yang[2], Jie Tian[1], Ping Xing[1], Hai-Ling Tang[1], Qian-Yi Qiu[1], Chang-Jun Wu[1]

Departments of [1]Ultrasound, [2]Endocrinology, First Affiliated Hospital of Harbin Medical University, Harbin, China

Received October 8, 2017; Accepted January 11, 2019; Epub April 15, 2019; Published April 30, 2019

Abstract: Objective: To investigate the diagnostic performance of qualitative shear wave elastography (SWE) in the characterization of thyroid nodules, compared with quantitative SWE and grayscale ultrasound (US). Methods: A total of 174 thyroid nodules from 174 patients were preoperatively evaluated by grayscale US and SWE. The quantitative SWE metrics were measured. For the qualitative SWE analysis, a four-pattern classification was established according to the color distribution features of the elastic maps and assigned for each enrolled nodule, as 1 for no meaningful findings, 2 for a capsule-related color, 3 for marginal color, and 4 for interior color. Results: Intra-observer and inter-observer agreement of the qualitative classification proposed in this study were substantial (κ=0.793 and 0.756, respectively). The area under the receiver operating characteristic curve (AUC) of the proposed classification was similar to that of grayscale US (P=0.73) and quantitative SWE metrics (P=0.90). Compared with the quantitative SWE, the qualitative classification yielded a higher sensitivity ($P < 0.05$) and a similar specificity (P=0.75). Adding SWE features to grayscale US, either qualitatively or quantitatively, improved the overall specificity (both $P < 0.001$). Among all data sets, the optimal diagnostic performance came from the combined set of grayscale US and the qualitative classification (AUC, 0.890), with 84.4% sensitivity and 94.6% specificity. Conclusion: The qualitative four-pattern classification proposed in this study was feasible and highly reproducible in the SWE evaluation of thyroid nodules. SWE imaging features, especially the qualitative classification, have the potential to facilitate ultrasound diagnosis for thyroid nodules.

Keywords: Ultrasound, shear wave elastography, thyroid nodule, diagnosis

Introduction

Ultrasound (US) is regarded as a first-line imaging method for the detection and identification of thyroid nodules. US elastography, a novel modality capable of revealing tissue biomechanical properties, has been recommended as an additional tool for conventional US for the diagnosis and management of thyroid nodules [1-3]. There are two main types of ultrasound elastography technologies that are frequently used, strain elastography and shear wave elastography [4]. Strain elastography (SE), the most widely used type of elastography, has been shown to be both highly sensitive and specific in the evaluation of thyroid nodules [5]. However, there are some intrinsic defects of SE, including high operator dependence and substantial interobserver variability [6, 7]. The diagnostic efficacy of SE has been challenged [8, 9].

Recently, shear wave elastography (SWE), a highly reproducible technique, has received increasing attention [10]. This system enables the generation of focused acoustic impulses to induce transverse shear waves, whose propagation velocities can be measured and used to deduce tissue stiffness quantitatively, expressed as either shear wave speed (m/s) or Young's modulus (kPa) [4, 11]. A growing number of studies shows promising applications of quantitative SWE in the differenti al diagnosis of thyroid nodules [10, 12-14]. However, the published thresholds for identifying thyroid cancers are fairly inconsistent, ranging from approximately 40 kPa to 90 kPa [13, 14]. There would be controversy with respect to introducing these results into clinical practice.

Quantitative assessment is not the only way to evaluate stiffness with the SWE technique. As confirmed by the literature, qualitative information provided by the color elastic map also helps in stiffness analysis [15-18]. Nonetheless, up until now, the value of qualitative SWE in the diagnosis of thyroid nodules has not been well established. One published study referring to this topic has proved the feasibility of qualitative SWE [19]. However, in their study, SWE images were assessed using Ueno and Rago scales, two widely utilized scoring systems for SE [20, 21]. Theoretically, there are many differences between SE and SWE, including the excitation methods and the measured physical quantities [4]. Moreover, SE images are generally analyzed according to the prevalence of 3 colors (e.g., red, blue, and green) [6, 22], whereas there are 6 main color levels in SWE images (i.e., black, dark blue, light blue, green, orange, red) [11]. These distinctions may lead to inaccuracy and confusion when we interpret SWE images using scoring systems for SE.

Therefore, the purpose of this study was to investigate the diagnostic performance of qualitative SWE in the differential diagnosis of thyroid nodules, compared with quantitative SWE and grayscale US.

Materials and methods

Patients

This retrospective study was approved by our Institutional Review Board, and written informed consent was waived. The methods in this study were performed in accordance with the approved study plan. From November 2016 to January 2017, 190 consecutive patients with thyroid nodules scheduled to undergo surgery were imaged by grayscale US and SWE. Among these included patients, sixteen were later excluded for the following reasons: six patients had previous invasive procedures for thyroid nodules, seven patients had cystic or almost cystic nodules, and three patients lacked histopathologic confirmation. One nodule per patient was included. For patients with multiple nodules, the most suspicious nodule on US or the largest one were selected for analysis. Ultimately, the study cohort consisted of 174 thyroid nodules in 174 patients. Surgical histopathologic results were used as the reference standard.

Image acquisition

Grayscale US and SWE imaging were performed using the same Aixplorer US instrument (SuperSonic Imagine, Aix-en-Provence, France) equipped with a 4-15 MHz linear-array transducer. All the examinations were performed by one of the two radiologists with more than 3 years of experience in US elastography. The patients were positioned in a supine position with their necks fully exposed.

The conventional US scanning was carried out according to the relevant practice guidelines [23]. Radiologists who performed the examination recorded nodule location and size (the maximal diameter measured on the US image). All grayscale US images were digitally stored for further analysis.

SWE images were acquired on a longitudinal plane following grayscale US by the same radiologist. When the SWE mode was activated, a rectangular field of view (FOV) was generated on the grayscale image, in which information of the tissue stiffness was obtained pixel by pixel and coded as a translucent color map ranging gradually from dark blue (soft) to red (stiff). During SWE data acquisition, the probe was kept stationary with minimal pressure. To reduce extra pre-compression, the FOV was first placed to include the anterior strap muscles of neck, and the patients were instructed to relax their necks, till the muscle layers were depicted without red/orange areas. At that point, the FOV was moved to include the target nodule. When the image was stable for several seconds, the operator froze and saved it for subsequent analysis. All SWE images were analyzed at the default color scale of 0-100 kPa.

Image analysis

The quantitative SWE was measured by the radiologist who performed the SWE imaging. The build-in circular region of interest (ROI) (Q-Box™; SuperSonic Imagine) was placed on the stiffest portion inside the nodule, taking care to avoid blood vessels, calcifications and cystic portions. The Q-box™ diameter was fixed at 2-mm in all cases. The SWE metrics of E_{max} (the maximum elastic modulus), E_{mean} (mean elastic modulus), E_{min} (minimum elastic mo dulus), and E_{SD} (elastic modulus standard devition) were automatically calculated.

The grayscale US and qualitative SWE features wer reviewed by another blinded radiologist with 6 years of experience in thyroid US. To reduce bias, the images were reviewed in a random order.

For each nodule, grayscale sonographic features including composition, echogenicity, margins, presence and type of calcifications, and shape were evaluated. Based on previous criteria, grayscale US features predictive of malig nancy were defined as marked hypoechgenicity (more hypoechoic compared with the adjacent strap mucle), poorly defined margin (a microlobulated or irregular margin), microcalcifications (tiny, punctate, hyperechoic foci without acoustic shadowing), and taller-than-wid shape [8, 24]. The nodules were classified as suspicious for malignancy when they had one or more of the malignant sonographic characteristics other wise, they were considered to beunsuspicious.

Qualitative SWE were evaluated visually, according to the color distribution features of the elastic maps. Here, the nodules were classified into four patterns (**Figure 1**). Pattern 1 (no meaningful findings) was assigned when no meaningful high stiffness color signal was revealed, including homogeneous blue, vertical strip artifacts [11, 17] and irregular color patces (**Figure 1A**). Pattern 2 (capsule-related color) was assigned to cases with areas coded in high stiffness color related to the thyroid capsules, which may extend to the interior of the nodule or the superficial cervical fascia (**Figure 1B**). Pattern 3 (marginal color) was assigned to cases with localized color signal at the nodule margin adjacent to thyroid parenchyma (**Figure 1C**). Pattern 4 (interior color) was assigned when localized colors were observed interior of the lesion heterogeneously (**Figure 1D**). The localized color described in pattern 3 and 4, in particular, refers to increased stiffness that neither continues as vertical bands beyond the nodule nor belongs to color patches that distribute diffusedly. Additionally, if a nodule indicated visual feature satisfying more than one patterns, the higher one was chosen (**Figure 2**). This four-pattern classification was modified from the criteria proposed by Tozaki et al. [17] for breast cancer (hereafter, the Tozaki criteria).

To evaluate the potential effect of adding SWE to grayscale US in predicting malignancy, combinations of grayscale US and SWE features were established, in which the thyroid nodules were divided into two categories. A nodule was classified as suspicious for malignancy when suspicious results were found by both grayscale US and SWE (i.e, greater than the cut-off value); otherwise, it would be classified as unsuspicious.

Observer agreement of the fourpattern classification

In a subset of 40 nodules, the observer agreement of the four-pattern classification was assessed. Three months after the first evaluation, the same radiologist reviewed the SWE images for intra-observer agreement calculation. Meanwhile, another two radiologists with 4 and 5 years of experience in thyroid US assessed all the elastograms separately, and the results were compared with each other for inter-observer agreement calculation.

Statistical analysis

The relevant findings on grayscale US and SWE were compared between the benign and malignant lesions. Categorical variables were compared using a chi-squared test and Fisher's exact test, while continuous variables were assessed using Student's *t* test. In addition, a Mann-Whitney U test was applied to compare continuous variables with a non-normal distribution. Receivers operating characteristic (ROC) curves were constructed for grayscale US, SWE features and the combined data sets. Areas under the ROC curve (AUC) were calculated and compared using a z test. For the SWE features, the optimal cut-off points to predict malignancy were determined using the Youden index (maximum of sensitivity+specificity-1). Sensitivity, specificity, accuracy, positive predictive values (PPVs) and negative predictive values (NPVs) were calculated for these cut-off points. Univariate and multivariate (logistic regression analysis) and odds ratios (OR) were calculated to determine independent predictors for thyroid malignancy. Inter-observer and intra-observer agreements were evaluated by cohen's κ statistic, and classified as slight (κ < 0.20), fair (κ=0.20-0.40), moderate (κ=0.40-0.60), substantial (κ=0.60-0.80), and almost perfect (κ=0.80-1.00) [25]. The statistical anal ysis was performed using the SAS software package (version 9.2, SAS Institute, Cary, NC). A two-tailed P < 0.05 was considered statisti-

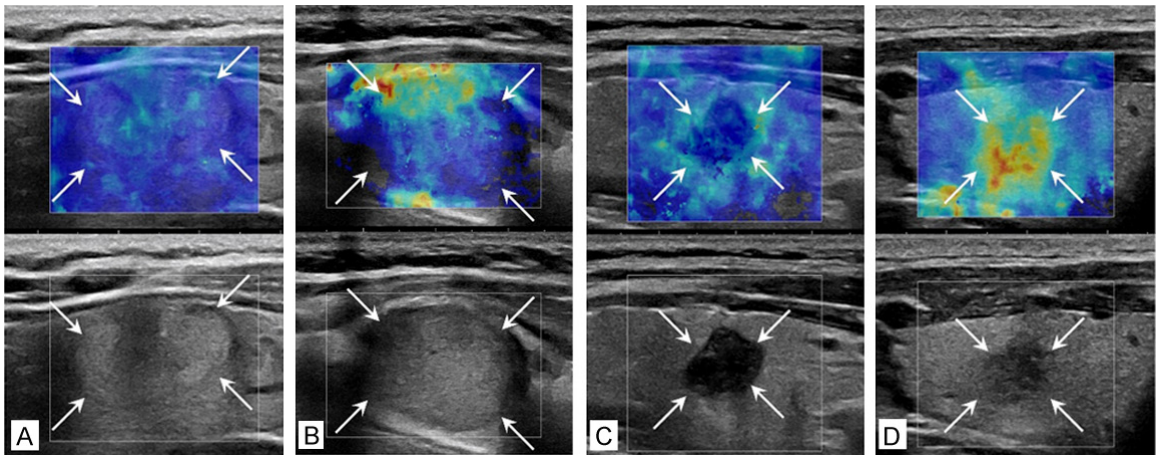

Figure 1. Representative images of the qualitative four-pattern classification. A. Scans of a nodular goiter (arrows). Shear wave elastography (SWE) image (top) is coded mostly blue with irregular cyan patches (no meaningful findings; pattern 1). B. Scans of a follicular adenoma (arrows). The SWE image (top) shows high stiffness areas related to capsules, extending to the intrinsic nodule tissues and the superficial cervical fascia (capsule-related color; pattern 2). C. Scans of a papillary thyroid carcinoma (arrows). SWE image (top) shows colored areas at the nodule margin adjacent to parenchyma (marginal color; pattern 3). D. Scans of a papillary thyroid carcinoma (arrows). Increased stiffness areas are present inside the nodule on SWE image (top) (interior color; pattern 4).

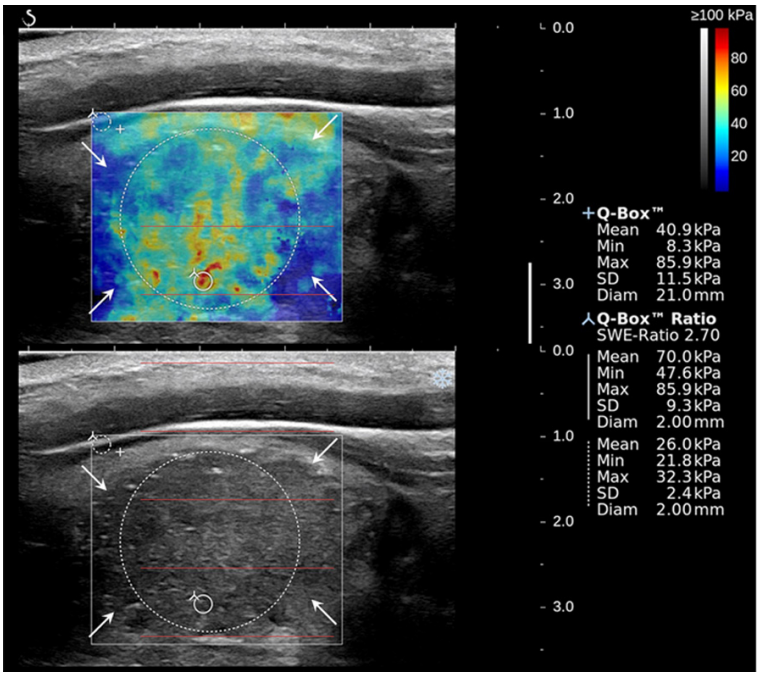

Figure 2. Papillary thyroid carcinoma (arrows) in an 18-year-old female patient. Grayscale image (bottom) shows a mass with a poorly defined margin and microcalcifications that were classified as suspicious for malignancy. The shear wave elastography (SWE) image (top) shows a qualitative feature satisfying pattern 2 (capsule-related color) and pattern 4 (interior color) simultaneously and the higher one, pattern 4 was chosen. The elasticity metric of E_{max} is 85.9 kPa.

cally significant, and 95% confidence intervals (CIs) were used.

Results

Demographic information and clinic features

A total of 174 patients (mean age, 47.4±10.5 years; range, 18-77 years) with 174 thyroid nodules (64 malignant, 110 benign) were evaluated in this study. These nodules underwent surgical excision mainly owing to the following reasons: biopsy-proven malignancy, compressive symptom, rapidgrowth, suspicion of malignancy, or patient anxiety. There were 140 women (mean age, 48.0±10.6 years; range, 18-77 years) and 34 men (mean age, 44.5±9.9 years; range, 20-58 years). Of the 174 thyroid nodules, 110 (63.2%) were benign and 64 (36.8%) were malignant. Amongst the demgraphic characteristics, age was associated with malignancy (P=0.001), but male sex was not (P=0.342). The histopathologic diagnoses are summarized in **Table 1**. The maximal diameter of the malignant nodules (14.4±12.7 mm; range, 3.7-78.0

Table 1. Histopathologic results of the 174 thyroid lesions

Histopathologic results		n
Benign	Nodular goiter	95
	Follicular adenoma	9
	Focal thyroiditis	4
	Others	2
Malignant	Papillary carcinoma	61
	Follicular carcinoma	1
	Medullar carcinoma	1
	Poorly differentiated carcinoma	1
Total		174

mm) was similar to the maximal diameter of the benign nodules (17.1±10.5 mm; range, 4.0-52.9 mm) (P=0.13).

Grayscale US features between benign and malignant nodules

Suspicious US features were more frequently seen in malignant nodules than benign nodules (all P < 0.001) (**Table 2**). The combined suspicious grayscale US features yielded an AUC of 0.813 (95% CI: 0.762, 0.864), and the corresponding sensitivity and specificity were 95.3%, 67.3%, respectively (**Table 3**).

Diagnostic performance of quantitative SWE

E_{mean}, E_{max}, E_{min} and E_{SD} weresinificantly higher in the malignant nodules than in benign nodules (P < 0.0001 for all) (**Table 2**). The diagnostic performances of the quantitative elasticity metrics are summarized in **Table 3**. Among all metrics, E_{max} yielded the highest AUC of 0.801 (95% CI: 0.732, 0.870), which showed no significant difference with that of grayscale US (P=0.79). At the optimal cut-off value of 52.1 kPa, a sensitivity of 73.4% and aspecificity of 76.4% were achieved. E_{max} was selected for the combined diagnosis.

Diagnostic performance of qualitative SWE classification

A significant difference was shown in the malignancy rate of the four-pattern classification (P < 0.001) (**Table 2**). The diagnostic performance of the qualitative classification is summarized in **Table 3**. The AUC value for the classification was 0.798 (95% CI: 0.731, 0.864), which was comparable to that of the grayscale US (P=0.73) and E_{max} (P=0.90) (**Figure 3A**). Using the optimal cut-off point between pattern 2 and 3, sensitivity and specificity was 89.1% and 74.6%, respectively. No significant difference was shown between the specificity of the qualitative classification and E_{max} (P=0.75), but the sensitivity of the classification was significantly higher (P=0.02) (**Figure 4**). **Table 4** shows the details of the 7 carcinomas misdiagnosed by both the qualitative and quantitative methods (**Figure 5**).

Observer agreement of the four-pattern classification

The intra-observer and inter-observer agreement of the classification were both substantial, with κ values of 0.793 and 0.756, respectively.

Diagnostic performance combined grayscale US and SWE for thyroid nodules

The corresponding diagnostic performances are shown in **Table 3**. Among all the data sets, the AUC of combination of US and the qualitative classification (US+pattern) was the highest, at 0.890 (95% CI: 0.840, 0.940), which was significantly higher than grayscale US alone (P=0.008) and US+E_{max} (P=0.024) (**Figure 3B**). Also, the difference in AUC between US and US+E_{max} was not significant (P=0.489). Adding SWE features to grayscale US, either qualitatively or quantitatively, improved the overall specificity (P < 0.0001 for both). There was no significant difference of sensitivity between grayscale US and US+pattern (P= 0.079), but the overall sensitivity for US+E_{max} decreased significantly (P=0.0003).

Univariate and multivariate regression analysis

At univariate logistic regression analysis, the presence of solitary nodule (OR: 2.219; 95% CI: 1.184, 4.156; P=0.013), E_{max} (OR: 8.932; 95% CI: 4.400, 18.131; P < 0.001) and qualitative classification (OR: 23.847; 95% CI: 9.748, 58.335; P < 0.001) were statistically significant predictors for thyroid malignancy, but gender (P=0.288) and nodule size (P=0.080) were not. On the other hand, older age (> 45 years; OR: 0.329; 95% CI: 0.171, 0.637; P=0.001) was predictive of thyroid benignity. At multivariate logistic regression analysis, the presence of a solitary nodule (OR: 2.692; 95% CI: 1.167,

Table 2. Grayscale US, qualitative SWE and quantitative SWE of benign and malignant thyroid nodules

	Pathology		P
	Malignancy (n=64)	Benign (n=110)	
Grayscale US*			
Marked hypoehogenicity	31 (48.4%)	8 (7.3%)	< 0.0001
poorly defined margin	36 (56.3%)	23 (20.9%)	< 0.0001
Microcalcification	41 (64.1%)	17 (15.5%)	< 0.0001
Taller-than-wide shape	20 (31.3%)	5 (4.6%)	< 0.0001
Qualitative classification*			< 0.0001
1- nomeaningful findings	6 (9.1%)	60 (90.9%)	
2- capsule-related color	1 (4.4%)	22 (95.7%)	
3- marginal color	24 (75.0%)	8 (25.0%)	
4- interior color	33 (62.3%)	20 (37.7%)	
Quantitative metrics(kPa)*			
E_{max}	75.20 (50.60, 113.95)	38.50 (29.10, 51.70)	< 0.0001
E_{mean}	64.70 (39.25, 90.65)	32.05 (23.30, 43.40)	< 0.0001
E_{min}	47.85 (23.65, 63.80)	23.75 (15.60, 32.30)	< 0.0001
E_{SD}	7.10 (4.75, 13.50)	3.70 (2.60, 5.90)	< 0.0001

Note: *Data in parenthesis are medians with interquartile ranges, otherwise percentages.

Table 3. Diagnostic performance of grayscale US, SWE, and US Combined with SWE in differentiating thyroid nodules

	Threshold	Sensitivity (%)	Specificity (%)	PPV (%)	NPV (%)	Accuracy (%)	AUC (95% CI)
Grayscale US	NA	95.3	67.3	62.9	96.1	77.6	0.813 (0.762-0.864)
Quantitative metrics (kPa)							
E_{max}	52.1	73.4	76.4	64.4	83.2	75.3	0.801 (0.732-0.870)
E_{mean}	44.1	68.8	77.3	63.8	81.0	74.1	0.791 (0.721-0.861)
E_{min}	35.3	64.1	80.0	65.1	79.3	74.1	0.763 (0.687-0.839)
E_{SD}	4.7	76.6	63.6	55.1	82.4	68.4	0.769 (0.697-0.841)
Qualitative classification	> 2	89.1*	74.6	67.1	92.1	79.9	0.798 (0.731-0.864)
US+E_{max}	NA	71.9**	95.5**	90.2	85.4	86.8	0.837 (0.778-0.896)
US+pattern	NA	84.4	93.6**	88.5	91.2	90.2	0.890 (0.8400-0.940)**,#

Note: AUC: area under the receiver operating characteristic curve; PPV: positive predict value; NPV: negative predict value; US: ultrasound; SWE: shear wave elastography; NA: not available; CI: confidence interval. *P < 0.05, in comparison with Quantitative metrics. **P < 0.05, in comparison with US only. #P < 0.05, in comparison with US+E_{max}.

6.211; P=0.020) and a qualitative classification (OR: 26.542; 95% CI: 10.151, 69.397; P < 0.001) were identified as independent predictors of thyroid malignancy, but E_{max} was excluded by the stepwise variable selection procedure (P=0.086). Likewise, older age (> 45 years; OR: 0.316; 95% CI: 0.133, 0.752; P=0.009) was identified to be an independent predictor for thyroid benignity.

Discussion

Quantitative SWE metrics have been used to evaluate thyroid nodules. Nevertheless, the optimal cut-off values in prior studies varied considerably. Liu et al. [13] proposed using an E_{mean} of 39.3 kPa, Kim et al. [24] proposed using E_{mean} at the higher level of 62 kPa, and Park et al. [14] proved that the optimal parameters for predicting malignancy were E_{mean} of 85.2 kPa and E_{max} of 94.0 kPa. This wide disparity could be ascribed to the different study designs, the inclusion and exclusion criteria, the scale of patient cohort, and the diverse proportion of malignancy among their study populations. Furthermore, the pre-compression level was not adequately standardized in

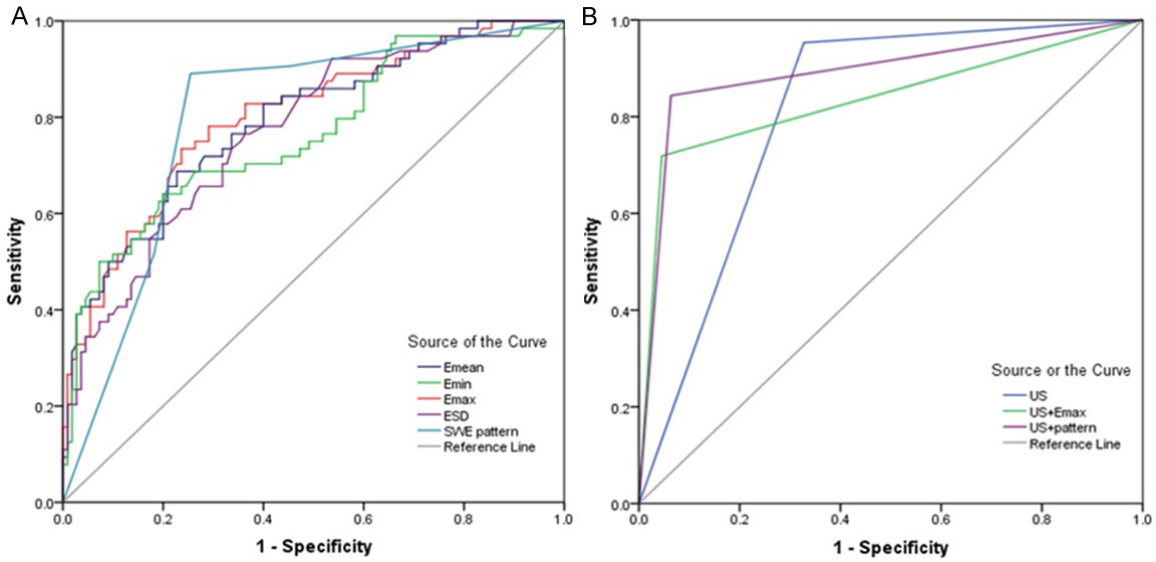

Figure 3. Receiver operating characteristic (roc) curves for all qualitative and quantitative SWE features (A) and US alone and US combined with SWE features (B).

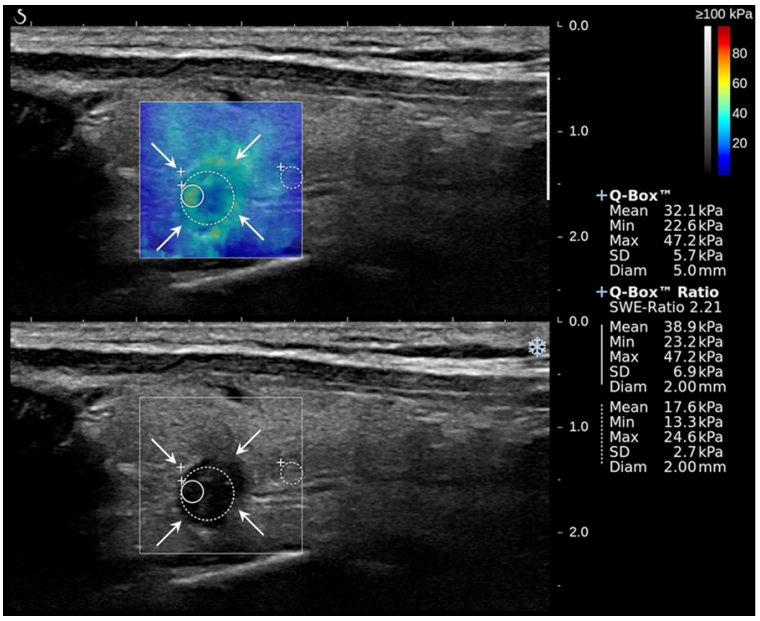

Figure 4. Papillary thyroid microcarcinoma (arrows) in a 47-year-old woman. The grayscale image (bottom) shows a nodule considered to be suspicious for malignancy. The shear wave elastography (SWE) image (top) shows increased stiffness signals at the marginal region considered to be pattern3, but with E_{max} lower than the cut-off value (52.1 kPa). This nodule was misdiagnosed by quantitative SWE.

published studies, which has been suggested as a possible factor influencing the results [26]. In our study, E_{max} showed the best diagnostic performance among all the quantitative SWE metrics, and the cut-off value (52.1 kPa) was within the range of those reported previously. Further studies with a larger population are necessary to determine the most appropriate quantitative metric in discriminating thyroid malignancy.

In previous studies, quantitative SWE features of thyroid nodules were obtained with the transducer orientated in different planes. Recently, Gangadhar et al. [27] reported that the diagnostic efficacy of thyroid nodule characterization was similar in both transverse and longitudinal orientations. Investigators have also adopted longitudinal planes to avoid potential artifacts generated by carotid, trachea and uneven acoustic forces distribution [10, 28]. Conversely, Samir et al. [29] indicated that the transverse plane was the optimal measurement plane to evaluate follicular-patterned thyroid lesions. In our clinical practice, howeer, we found it difficult to summarize certain qualitative patterns using SWE images obtained in transverse planes. Compared with longitudinal planes, anatomic structures in transverse planes are more complicated, and vary obviously as the transducer moves, which

Table 4. False-negative cases according to both qualitative and quantitative SWE

Case	Sex	Age	Suspicious grayscale features*	E_{max} value (kPa)	Qualitative classification	Maximal diameter (mm)	Pathology
1	F	45	1	34.3	1	6.8	PTMC
2	F	46	3	24.0	1	3.2	PTMC
3	F	38	4	30.9	1	4.2	PTMC
4	F	35	2	25.4	1	8.7	PTMC
5	F	44	3	29.9	2	7.1	PTMC
6	F	45	3	28.7	1	6.5	PTMC
7	F	27	2	32.3	1	9.3	PTMC

Note: PTMC: papillary thyroid microcarcinoma; FTC: follicular thyroid carcinoma. *Number of suspicious grayscale features.

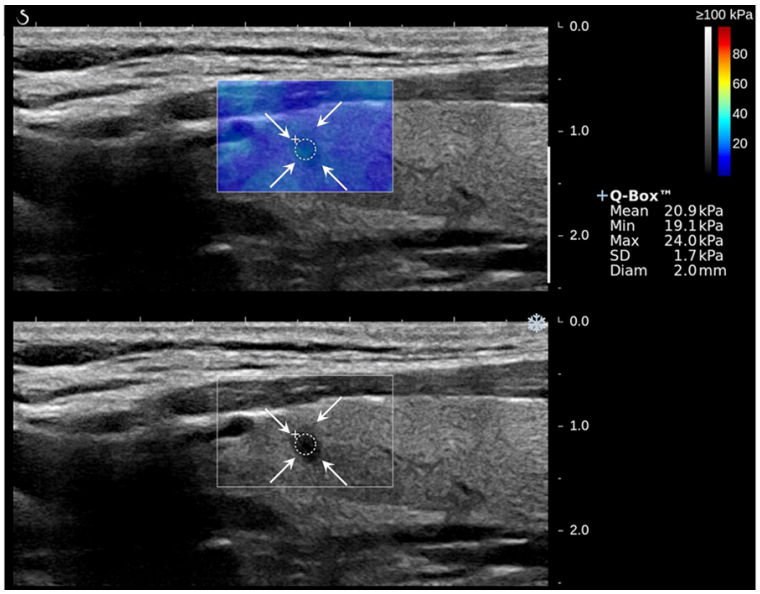

Figure 5. Scans of Case 2 in **Table 4**, a surgery-proven papillary thyroid microcarcinoma (arrows). It is a nodule considered to be suspicious on grayscale image (bottom), but negative on both quantitative and qualitative shear wave elastography (SWE) (top). The SWE image shows the nodule and the surrounding tissue coded homogeneously blue (pattern 1), with an E_{max} of 24.0 kPa.

in turn leads to various visual features in the elastograms. In the present study, therefore, the longitudinal plane was selected to acquire all the SWE images.

For qualitative SWE assessment, we categorized the lesions into four patterns, which were modified from the Tozaki criteria [17]. The vertical stripe artifact, a separate pattern in the Tozaki criteria, is frequently observed in superficial breast lesions [11]. However, we found it relatively rare for the thyroid. This might be caused by the disparate anatomic characteristics bet-ween the thyroid and the breasts, or the different imaging settings. Wehence integrated the vertical stripe artifact in to a pattern 1 (no meaningful findings). Pattern 2 (capsule-relatedcolor) could be seen in nodules close to the thyroid capsules, especially the large ones that protruded from the anterior or posterior aspect of thyroid lobe. We speculated this may represent a high stress state of the thyroid capsules, since these nodules are somewhat restricted by the thyroid capsules and the cervical soft tissue. The marginal region of stiffness depicted in pattern 3 (marginal color) has been previously emphasized in the diagnosis of breast lesions [30, 31]. It is also suggestive of thyroid malignancy, which may be explained as marginal tumor infiltration or desmoplastic reaction. Besides, cancerous tissues are generally harder than benign ones [10, 13], and tend to appear as interior stiff areas which correspond to pattern 4 (interior color).

Multivariate logistic regression indicated that the proposed qualitative classification was an independent predictor for thyroid malignancy. As compared with quantitative metrics, the proposed classification showed a similar diagnostic performance (P=0.90) and specificity (P=0.75), while the sensitivity was significantly higher (P=0.02). Notably, with the cut-off point set between pattern 2 and 3, eight of fifteen carcinomas omitted by E_{max} were detected by the proposed classification (**Figure 4**). These were mostly small nodules measured to be "soft" (Young's modulus below the cut-off E_{max}

of 52.1 kPa), but with patterns indicating malignancy. The qualitative SWE features, moreover, can be assessed independent of the numerical cut-off values, which were inconsistent as discussed earlier. Additionally, our results indicated that the four-pattern classification was highly reproducible with substantial intra-observer and inter-observer agreement. Therefore, in thyroid SWE, the proposed classification could serve as a time-saving and practical evaluation method for differential diagnosis.

In this study, all malignant nodules misclassified by both quantitative and qualitative SWE were papillary thyroid carcinomas (PTC) with maximal diameters ≤ 10 mm, namely, papillary thyroid microcarcinomas (PTMCs) (**Table 4**). This implied a suboptimal power of SWE in detecting PTMC, a finding compatible with previous results [13, 32]. The cause of this phenomenon is unclear. One possibility is that PTMC is soft due to its genetic and biological properties [13]. The soft appearance of these PTMCs, however, might also be spurious and partially related to technical limitations, such as the slightly poorer spatial resolution and/or an insufficient generation of regular shear waves in small nodules [33, 34]. Further study is needed to elucidate this topic. On the other hand, all the PTMCs misdiagnosed by the SWE method were categorized as suspicious on grayscale US. A comprehensive interpretation of B-mode findings and elastographic features is necessary for small nodules.

Previous studies have confirmed that the combination of conventional US and elastography could achieve better performance in detecting thyroid malignancy [12, 35, 36]. Nevertheless several studies have also reported limited additional value of quantitative SWE parameters as compared to conventional US alone [32, 37]. Similarly, in the present study, diagnostic performance of US were not significantly improved by adding E_{max} (P=0.489). The combination of the qualitative classification and grayscale US, however, yielded the highest AUC among all data sets, which was significantly higher than that of conventional US (P=0.008) or the combined data of US and E_{max} (P=0.024). Our results also revealed that adding SWE features to grayscale US, either qualitatively or quantitatively, yielded higher specificity than US alone (P < 0.001 for both).

There were some limitations to our study. First, all the SWE images were analyzed at the default color scale. However, color contrast will vary with the adjustment of the scale, by which further qualitative information about stiffness might be obtained [31]. Second, assessment based on a visual method is subjective, but in our study, a substantial observer agreement of the proposed classification was found. In the future, by using computer-aided-diagnosis systems, more meaningful results might be achieved [26]. Third, this is a retrospective study, and the patients enrolled were scheduled for thyroid surgery, so our results may be influenced by sampling bias. Fourth, the sample size of this preliminary study is relatively small, so a subgroup analysis of the pathological type was precluded. In addition, potential influencing factors for SWE measurements and classifications, such as the presence of calcifications, lesion position, and cystic change were not considered in our study [13, 37, 38].

Conclusions

Our initial study revealed that qualitative SWE assessed by the proposed four-pattern classification is feasible in thyroid nodule characterization. Compared with quantitative SWE, qualitative SWE offers a comparable diagnostic performance with a higher sensitivity, so it may represent SWE in clinical practice. SWE features, especially the qualitative classification, have the potential to be valuable adjuncts to conventional US. However, further studies are warranted to validate our results.

Acknowledgements

This work was supported by grants 81271-648 and 81671697 from the National Natural Science Foundation of China.

Disclosure of conflict of interest

None.

Address correspondence to: Chang-Jun Wu, Department of Ultrasound, First Affiliated Hospital of Harbin Medical University, 23 Youzheng Road, Harbin, Heilonjiang, China. Tel: (+86-451)85555905; E-mail: changjunwu1964@hotmail.com

References

[1] Cosgrove D, Barr R, Bojunga J, Cantisani V, Chammas MC, Dighe M, Vinayak S, Xu JM, Di etrich CF. WFUMB guidelines and recommen dations on the clinical use of ultrasound elas tography: part 4 thyroid. Ultrasound Med Biol 2017; 43: 4-26.

[2] Gharib H, Papini E, Garber JR, Duick DS, Har rell RM, Hegedüs L, Paschke R, Valcavi R, Vitti P; AACE/ACE/AME Task Force on Thyroid Nod ules. American association of clinical endocri nologists, american college of endocrinology, and associazione medici endocrinologi medi cal guidelines for clinical practice for the diag nosis and management of thyroid nod ules--2016 update. Endocr Pract 2016; 22: 622-639.

[3] Cosgrove D, Piscaglia F, Bamber J, Bojunga J, Correas JM, Gilja OH, Klauser AS, Sporea I, Cal liada F, Cantisani V, D'Onofrio M, Drakonaki EE, Fink M, Friedrich-Rust M, Fromageau J, Havre RF, Jenssen C, Ohlinger R, Saftoiu A, Schaefer F, Dietrich CF, Efsumb. EFSUMB guidelines and recommendations on the clini cal use of ultrasound elastography. part 2: clinical applications. Ultraschall Med 2013; 34: 238-253.

[4] Shiina T, Nightingale KR, Palmeri ML, Hall TJ, Bamber JC, Barr RG, Castera L, Choi BI, Chou YH, Cosgrove D, Dietrich CF, Ding H, Amy D, Farrokh A, Ferraioli G, Filice C, Friedrich-Rust M, Nakashima K, Schafer F, Sporea I, Suzuki S, Wilson S and Kudo M. WFUMB guidelines and recommendations for clinical use of ultra sound elastography: part 1: basic principles and terminology. Ultrasound Med Biol 2015; 41: 1126-1147.

[5] Razavi SA, Hadduck TA, Sadigh G and Dwame na BA. Comparative effectiveness of elasto graphic and B-mode ultrasound criteria for di agnostic discrimination of thyroid nodules: a meta-analysis. AJR Am J Roentgenol 2013; 200: 1317-1326.

[6] Cantisani V, Grazhdani H, Drakonaki E, D'Andrea V, Di Segni M, Kaleshi E, Calliada F, Catalano C, Redler A, Brunese L, Drudi FM, Fu marola A, Carbotta G, Frattaroli F, Di Leo N, Cic cariello M, Caratozzolo M and D'Ambrosio F. Strain US elastography for the characterization of thyroid nodules: advantages and limitation. Int J Endocrinol 2015; 2015: 908575.

[7] Park SH, Kim SJ, Kim EK, Kim MJ, Son EJ and Kwak JY. Interobserver agreement in assess ing the sonographic and elastographic fea tures of malignant thyroid nodules. AJR Am J Roentgenol 2009; 193: W416-423.

[8] Moon HJ, Sung JM, Kim EK, Yoon JH, Youk JH, Kwak JY. Diagnostic performance of gray-scale US and elastography in solid thyroid nodules. Radiology 2012; 262: 1002-1013.

[9] Unlütürk U1, Erdoğan MF, Demir O, Güllü S, Başkal N. Ultrasound elastography is not supe rior to grayscale ultrasound in predicting malig nancy in thyroid nodules. Thyroid 2012; 22: 1031-1038.

[10] Veyrieres JB, Albarel F, Lombard JV, Berbis J, Sebag F, Oliver C and Petit P. A threshold value in shear wave elastography to rule out malig nant thyroid nodules: a reality? Eur J Radiol 2012; 81: 3965-3972.

[11] Berg WA, Cosgrove DO, Dore CJ, Schafer FK, Svensson WE, Hooley RJ, Ohlinger R, Mendel son EB, Balu-Maestro C, Locatelli M, Tourasse C, Cavanaugh BC, Juhan V, Stavros AT, Tardivon A, Gay J, Henry JP, Cohen-Bacrie C, Investiga tors BE. Shear-wave elastography improves the specificity of breast US: the BE1 multinational study of 939 masses. Radiology 2012; 262: 435-449.

[12] Sebag F, Vaillant-Lombard J, Berbis J, Griset V, Henry JF, Petit P and Oliver C. Shear wave elas tography: a new ultrasound imaging mode for the differential diagnosis of benign and malig nant thyroid nodules. J Clin Endocrinol Metab 2010; 95: 5281-5288.

[13] Liu B, Liang J, Zheng Y, Xie X, Huang G, Zhou L, Wang W and Lu M. Two-dimensional shear wave elastography as promising diagnostic tool for predicting malignant thyroid nodules: a prospective single-centre experience. Eur Ra diol 2015; 25: 624-634.

[14] Park AY, Son EJ, Han K, Youk JH, Kim JA and Park CS. Shear wave elastography of thyroid nodules for the prediction of malignancy in a large scale study. Eur J Radiol 2015; 84: 407-412.

[15] Youk JH, Son EJ, Gweon HM, Kim H, Park YJ and Kim JA. Comparison of strain and shear wave elastography for the differentiation of be nign from malignant breast lesions, combined with B-mode ultrasonography: qualitative and quantitative assessments. Ultrasound Med Biol 2014; 40: 2336-2344.

[16] Cong R, Li J and Guo S. A new qualitative pat tern classification of shear wave elastograghy for solid breast mass evaluation. Eur J Radiol 2017; 87: 111-119.

[17] Tozaki M and Fukuma E. Pattern classification of ShearWave Elastography images for differ ential diagnosis between benign and malig nant solid breast masses. Acta Radiol 2011; 52: 1069-1075.

[18] Guibal A, Boularan C, Bruce M, Vallin M, Pilleul F, Walter T, Scoazec JY, Boublay N, Dumortier J and Lefort T. Evaluation of shearwave elastog raphy for the characterisation of focal liver le sions on ultrasound. Eur Radiol 2013; 23: 1138-1149.

[19] Szczepanek-Parulska E, Wolinski K, Stangier ski A, Gurgul E, Biczysko M, Majewski P, Rewaj-Losyk M and Ruchala M. Comparison of diag-

nostic value of conventional ultrasonography and shear wave elastography in the prediction of thyroid lesions malignancy. PLoS One 2013; 8: e81532.
[20] Itoh A, Ueno E, Tohno E, Kamma H, Takahashi H, Shiina T, Yamakawa M and Matsumura T. Breast disease: clinical application of US elastography for diagnosis. Radiology 2006; 239: 341-350.
[21] Rago T, Scutari M, Santini F, Loiacono V, Piaggi P, Di Coscio G, Basolo F, Berti P, Pinchera A and Vitti P. Real-time elastosonography: useful tool for refining the presurgical diagnosis in thyroid nodules with indeterminate or nondiagnostic cytology. J Clin Endocrinol Metab 2010; 95: 5274-5280.
[22] Friedrich-Rust M, Vorlaender C, Dietrich CF, Kratzer W, Blank W, Schuler A, Broja N, Cui XW, Herrmann E and Bojunga J. Evaluation of strain elastography for differentiation of thyroid nodules: results of a prospective DEGUM multicenter study. Ultraschall Med 2016; 37: 262-270.
[23] American Institute of Ultrasound in Medicine; American College of Radiology; Society for Pediatric Radiology; Society of Radiologists in Ultrasound. AIUM practice guideline for the performance of a thyroid and parathyroid ultrasound examination. J Ultrasound Med 2013; 32: 1319-1329.
[24] Kim H, Kim JA, Son EJ and Youk JH. Quantitative assessment of shear-wave ultrasound elastography in thyroid nodules: diagnostic performance for predicting malignancy. Eur Radiol 2013; 23: 2532-2537.
[25] Landis JR and Koch GG. The measurement of observer agreement for categorical data. Biometrics 1977; 33: 159-174.
[26] Bhatia KS, Lam AC, Pang SW, Wang D and Ahuja AT. Feasibility study of texture analysis using ultrasound shear wave elastography to predict malignancy in thyroid nodules. Ultrasound Med Biol 2016; 42: 1671-1680.
[27] Gangadhar K, Hippe DS, Thiel J and Dighe M. Impact of image orientation on measurements of thyroid nodule stiffness using shear wave elastography. J Ultrasound Med 2016; 35: 1661-1667.
[28] Meng W, Xing P, Chen Q and Wu C. Initial experience of acoustic radiation force impulse ultrasound imaging of cervical lymph nodes. Eur J Radiol 2013; 82: 1788-1792.
[29] Samir AE, Dhyani M, Anvari A, Prescott J, Halpern EF, Faquin WC and Stephen A. Shear-wave elastography for the preoperative risk stratification of follicular-patterned lesions of the thyroid: diagnostic accuracy and optimal mesurement plane. Radiology 2015; 277: 565-573.
[30] Gweon HM, Youk JH, Son EJ and Kim JA. Visually assessed colour overlay features in shear-wave elastography for breast masses: quantification and diagnostic performance. Eur Radiol 2013; 23: 658-663.
[31] Zhou J, Zhan W, Chang C, Zhang X, Jia Y, Dong Y, Zhou C, Sun J and Grant EG. Breast lesions: evaluation with shear wave elastography, with special emphasis on the “stiff rim” sign. Radiology 2014; 272: 63-72.
[32] Wang F, Chang C, Gao Y, Chen YL, Chen M and Feng LQ. Does shear wave elastography provide additional value in the evaluation of thyroid nodules that are suspicious for malignancy? J Ultrasound Med 2016; 35: 2397-2404.
[33] Bamber J, Cosgrove D, Dietrich CF, Fromageau J, Bojunga J, Calliada F, Cantisani V, Correas JM, D’Onofrio M, Drakonaki EE, Fink M, Friedrich-Rust M, Gilja OH, Havre RF, Jenssen C, Klauser AS, Ohlinger R, Saftoiu A, Schaefer F, Sporea I and Piscaglia F. EFSUMB guidelines and recommendations on the clinical use of ultrasound elastography. Part 1: basic principles and technology. Ultraschall Med 2013; 34: 169-184.
[34] Fukuhara T, Matsuda E, Endo Y, Takenobu M, Izawa S, Fujiwara K and Kitano H. Correlation between quantitative shear wave elastography and pathologic structures of thyroid lesions. Ultrasound Med Biol 2015; 41: 2326-2332.
[35] Xing P, Chen Q, Yang ZW, Liu CB and Wu C. Combination of conventional ultrasound and tissue quantifcation using acoustic radiation force impulse technology for differential diagnosis of small thyroid nodules. Int J Clin Exp Med 2016; 9: 8288-8295.
[36] Liu Z, Jing H, Han X, Shao H, Sun YX, Wang QC and Cheng W. Shear wave elastography combined with the thyroid imaging reporting and data system for malignancy risk stratification in thyroid nodules. Oncotarget 2017; 8: 43406-43416.
[37] Dobruch-Sobczak K, Zalewska EB, Guminska A, Slapa RZ, Mlosek K, Wareluk P, Jakubowski W and Dedecjus M. Diagnostic performance of shear wave elastography parameters alone and in combination with conventional b-mode ultrasound parameters for the characterization of thyroid nodules: a prospective, dual-center study. Ultrasound Med Biol 2016; 42: 2803-2811.
[38] Szczepanek-Parulska E, Wolinski K, Stangierski A, Gurgul E, Ruchala M. Biochemical and ultrasonographic parameters influencing thyroid nodules elasticity. Endocrine 2014; 47: 519-527.